Chapter 9
Load Spectra

9.1 Introduction

The fatigue loads on a structure in service are generally referred to as the load spectrum. The description of load spectra and methods to obtain load spectra are discussed in the present chapter. A survey of various aspects of fatigue of structures was presented as a flow diagram in introductory chapter (Chapter 1, Figure 1.2). A reduced diagram is presented here in Figure 9.1 to illustrate the significance of load spectra for fatigue design analysis of a structure. Without information on the anticipated load spectrum, the analysis of the fatigue performance of a structure is impossible. Furthermore, verification tests to support the analysis are often necessary for economic or safety reasons. The load spectrum must be consulted for planning such validation tests.

Sometimes the load spectrum is changed after a number of years by a modified use of the structure, which is different from the initial expectations. The load spectrum must then be considered again. Fatigue load spectra should also be reviewed if fatigue failures occur in service.

The load spectrum of a structure should give information about the load-time history, which is the variation of the load as a function of time,

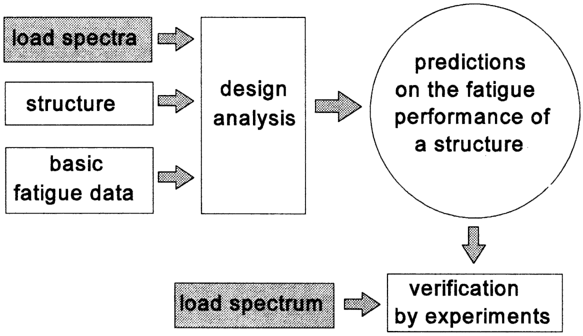

Fig. 9.1 Load spectra as input for the fatigue performance of a structure.

$P(t)$. The present knowledge of the fatigue phenomenon as it occurs in technical materials (see Chapter 2) clearly indicates that the significant points of a $P(t)$ load history are the maxima and minima, P_{max} and P_{min}, see Figure 9.2. At these load levels, reversal of cyclic slip occurs in the material, either at the material surface or in the crack tip plastic zone. These reversals are decisive for the fatigue damage accumulation in a structure. Several practical questions arise:

1. Is it necessary to know the full sequence of all turning points of the load history?
2. Are all similar structures in service subjected to the same load history, or in other words, how unique is a certain load history for a structure?
3. Are small cycles of interest, or is the fatigue damage contribution of these cycles negligible?
4. Is it important whether loads are applied at a high or a low loading rate (wave shape)?
5. Long periods at zero load (rest periods, structure not in use) or long periods at a significant load level (average load in service if dynamic

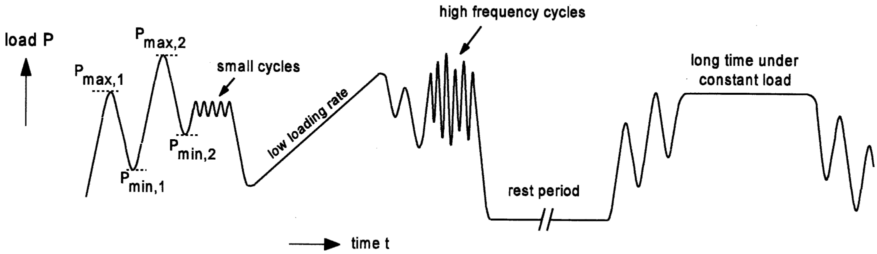

Fig. 9.2 Characteristic occurrences of a load-time history $P(t)$.

loads do not occur during that period), are these periods important for the fatigue damage accumulation?

The last two questions are pointing to problems of time dependent phenomena, e.g. corrosion, creep, or diffusion processes in the material which might affect the fatigue process. In the literature, these problems are frequently discussed as effects of the load frequency (cycles per minute) and the cyclic wave shape, see Section 2.5.7 (e.g. Figure 2.30).

Before the above problems can be discussed, an essential question is: Is the load history known which a structure will experience in service, or can it be estimated? Even more, how can the load history be described, and can it be measured? In the present chapter, load histories of different types of structure are discussed first (Section 9.2), which reveals essential differences between the statistical nature of load histories. Methods for the description of a load history and statistical compilations of load spectrum data are presented in Section 9.3. The determination of load spectra is discussed in Section 9.4. Service-simulation load histories are addressed in Section 9.5. The major aspects of the present chapter are summarized in Section 9.6.

9.2 Different types of loads on a structure in service

Which loads occur on a structure in service?
Answers to this question depend on the type of structure and how the structure is used. First some exemplary cases are discussed in a qualitative way to illustrate the variety of problem settings. Different types of loads can then be defined.

1. *Pressure vessel*
Many pressure vessels used in the industry and other production facilities are used in a simple way. The pressure is built up to a specific working level, maintained at that level, and then released to zero. If such a pressure cycle occurs about five times a day, the load spectrum contains approximately 40000 cycles in a life period of 20 years. Fatigue problems could arise. A number of questions can easily be formulated. Is the pressure always the same. Are the number of pressurization cycles user dependent? Is the duration of a pressure cycle important? Is the gas or liquid inside the pressure vessel aggressive? Anyhow, a number of questions to be considered if fatigue critical notches, usually inlets and joints, occur in the pressure vessel.

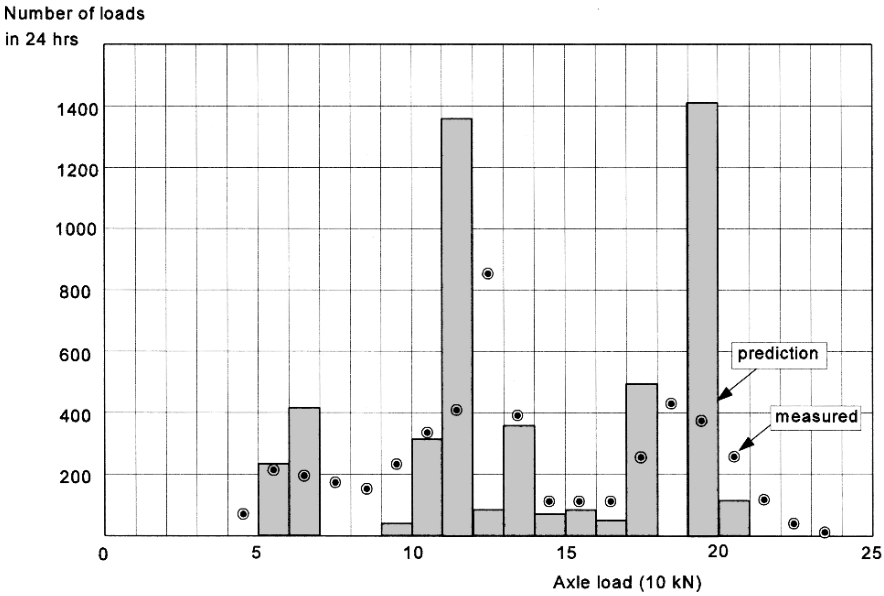

Fig. 9.3 (a) Axle loads on a railway bridge in 10 kN intervals.

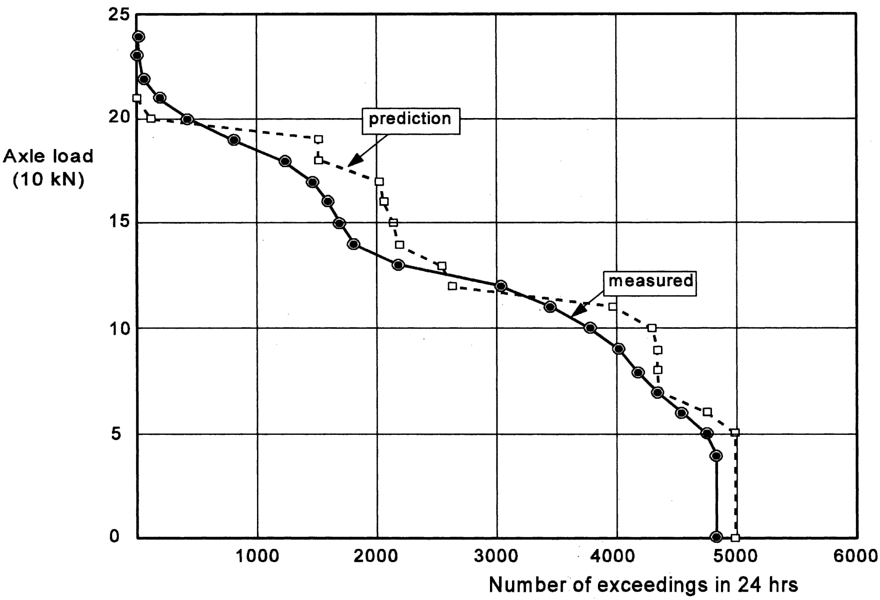

Fig. 9.3 (b) Load spectrum of axle load level exceedings for data in Figure 9.3a.

2. *Bridge*

The variety of bridges is large. A simple steel railway bridge is considered here. It is loaded in bending by each passage of a train. The load spectrum in a specific case of the Dutch Railways was depending on the number of train axles passing the bridge each day and the weight applied by the axles to the bridge. The load spectrum was predicted by considering the variety of trains that would use the bridge [1]. The prediction is shown as a bar chart (histogram) in Figure 9.3a, which gives the number of axle loads in intervals of 10 kN. The load spectrum was checked later, see the measured data in Figure 9.3a. It turns out that the scatter of the axle loads was larger than predicted. The same data are compared in Figure 9.3b by plotting the numbers of load level exceedings, i.e. the number of times that a specific load level is exceeded in 24 hours. Low load levels are exceeded many times, while high load levels occur less frequently. The results in Figure 9.3b show a reasonable agreement between the measured data and predictions. Some agreement should be present if the utilization of a structure is well defined and known in advance. This applies to the example of Figure 9.3 of trains used in accordance with a specified time table. However, for other moving vehicles such a prediction can be more difficult.

3. *Lamp post*

Modern aluminium street light posts are predominantly loaded by wind forces coming from different directions and varying intensities. For a lamp post as shown in Figure 9.4, it leads to bending and torsion load cycles with maxima stress levels near the base of the pillar. Usually, an opening is made in the pillar close to the base for making electrical connections. Although a cover is closing the opening, stress concentrations are present in that area and fatigue cracks have occurred. A correlation between the function of the street light and load spectrum does not exist. The load spectrum depends on the weather conditions, which should be described in statistical terms. Weather conditions depend on the geographical location. These conditions can be more severe along a sea cost where humidity and salt concentration can also adversely affect the fatigue behavior. Another obvious aspect involved is the dynamic response of the pillar on the wind fluctuations. It cannot be expected that the wind load spectrum on the street light and the stress spectrum at the fatigue critical location are linearly related. Dynamic response calculation techniques are well developed, but it may be advisable to measure the stress spectrum on a representative location of the structure.

Fig. 9.4 Lamp post in Pijnacker (the Netherlands).

4. *Motor-car* The load spectrum on a car can be very complex. It obviously depends on two major inputs: (i) the driver, and (ii) the condition of the roads to be used. A single load spectrum applying to all cars of the same type is impossible. Moreover, an average load spectrum applicable to most cars is meaningless. Fatigue failures are associated with severe driving and poor roads which applies to a small percentage of cars. However, a small percentage is still a large number of cars. It implies that a relatively severe load spectrum must be considered for the fatigue performance. The fatigue problem of motor-cars is also associated with the complexity of the structure with several components which can be fatigue critical. In addition, loads on a car act on the wheels in three different directions (x, y, z) with different frequencies and phase angles. Inertial forces on the flexible structure are also complex. All these conditions imply that a load spectrum cannot easily be defined. It is for these reasons that the motor-car industry is relying on experience, measurements and experiments.

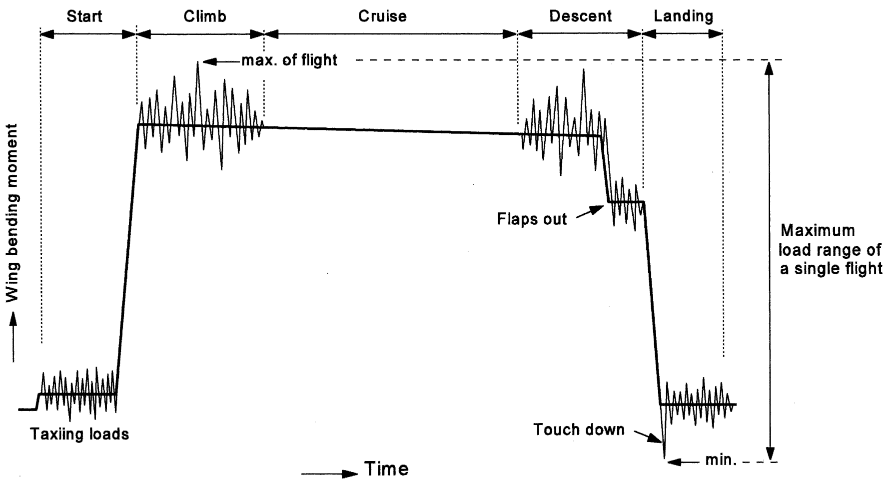

Fig. 9.5 Slow load variation of the wing bending moment during a single flight, with fast superimposed turbulence loads and ground loads.

5. *Wing of transport aircraft*
The aerodynamic lift on the wing of an aircraft is carrying the aircraft weight. The distributed lift on the wing exerts a bending moment with a maximum at the root of the wing. On the ground, the lift is zero and the aircraft is supported by the undercarriage. Each flight thus implies a cycle of the bending moment on the wing, see the heavy line in Figure 9.5. Bending of the wing introduces tension stresses in the lower wing skin structure and compression in the upper wing skin structure. The tension skin is well recognized as a fatigue critical part of the wing. The once per flight cycle on the tension skin is a very slow cycle with an almost quasi-static variation of the load. However, the wing is also subjected to much faster load cycles, see Figure 9.5. In flight, these cycles occur in turbulent air (gusty weather) predominantly during the climb and descent period at low altitudes. The turbulence at cruising altitude is usually very limited, and load variations are small (a small change due to fuel consumption). Also maneuver loads can be significant, depending on the type of aircraft. During take-off and landing, high-frequency cycles are introduced by runway roughness, touch-down on the ground, and spin up of the wheels. In addition to wing bending, torsional moments are also exerted on the wing. The loading picture is fairly complex, which is only schematically illustrated by Figure 9.5.

The above examples illustrate a variety of different loads. Two major types of characteristic groups of loads must be recognized:

1. Deterministic loads.
2. Stochastic loads.

A load is considered to be deterministic if it can be defined as a specific occurrence, from which it is known that it will occur with a magnitude that can be estimated. Deterministic loads should follow from the planned utilization of a structure. The load cycle of a pressure vessel is fully deterministic. Manoeuvers of ships and transport aircraft are predominantly deterministic. Many loads on a motor-car, a bridge, or a crane are predictable and have a deterministic character. However, depending on how such structures are used, loads cannot always be considered to be deterministic. Obviously, joyriding a car can lead to unpredictable loads.

Stochastic loads have an essentially statistical nature. They cannot be predicted to occur with a certain magnitude at a given moment. Good examples are wind forces on a street light pillar, forces exerted by waves of the sea on ships and drilling platforms, turbulence on an aircraft, and loads on motor-cars due to poor road conditions. A description of stochastic loads can only be done in a statistical way, i.e. in terms of the probability that something will happen. Stochastic loads are also referred to as random loads. In many cases, the statistical properties of stochastic loads are not very well known, although long-term measurements have provided useful data, e.g. for sea waves and wind forces.

Stochastic and deterministic loads can also occur simultaneously on the same structure. An example is shown in Figure 9.5 with random turbulence and runway roughness loads superimposed on the deterministic once-per-flight load cycle. The problem is how to combine these loads for fatigue evaluations. The superimposed loads increase the severity of the flight because the maximum load occurring during a flight becomes more severe, and the same is true for the minimum load. This aspect will be reconsidered in the following section on describing load histories.

Another aspect of random loads is that the intensity is not always the same. The statistical properties are not necessarily constant. This is easily understood by considering random loads depending on the weather conditions. Stormy weather can induce severe random loads on a lamp post, but more frequently occurring milder weather conditions can also contribute to fatigue. It has led to a second differentiation between load histories:

(i) Stationary load histories.
(ii) Non-stationary load histories.

In the first case, the statistical properties do not vary as a function of time, whereas in the second case, these properties can vary during the service

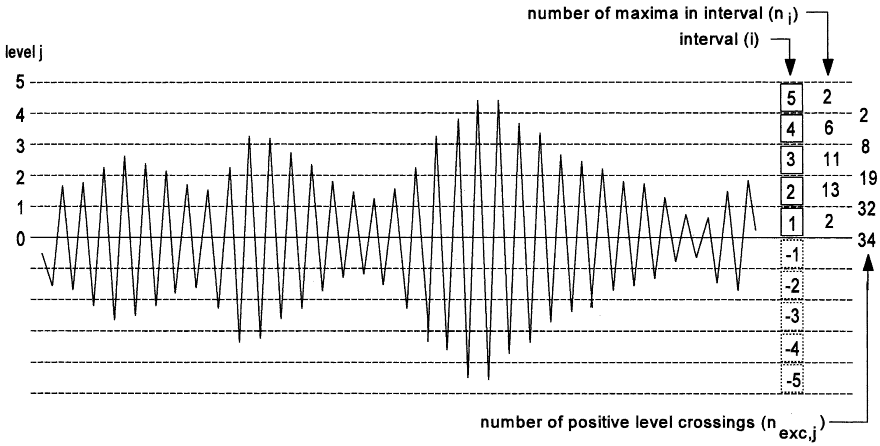

Fig. 9.6 Results of counting maxima of a symmetric load time history (varying amplitude).

usage of a structure. Although the terms stationary and non-stationary load histories are usually associated with stochastic loads, they can also apply to deterministic loads, e.g. by changing the use of a structure.

9.3 Description of load histories

Level crossing count methods

A load-time history is defined by a sequence of maxima and minima if time-dependent phenomena are not considered: $P_{\max,1}$, $P_{\min,1}$, $P_{\max,2}$, $P_{\min,2}$, etc. Such a sequence is usually reduced to a statistical representation in order to have a useful survey of the fatigue loads. In the past, several counting techniques were developed for this purpose based on counting level crossings for a number of load levels or counting peak values above a number of load levels. The historical development (see [2]) will not be followed here, but basic aspects of statistical count procedures are considered.

A simple load sequence is shown in Figure 9.6, a load signal with a varying amplitude. Approximately similar maxima and minima occur around a mean level, indicated as level 0. In view of the symmetry around this level, it is sufficient to consider the maxima only. Usually, load spectra are presented as numbers of peak values occurring above a load level j denoted as $n_{\text{exc},j}$. In the present case, this number is equal to the number of positive level crossings (going from a minimum to a maximum) of load level j.

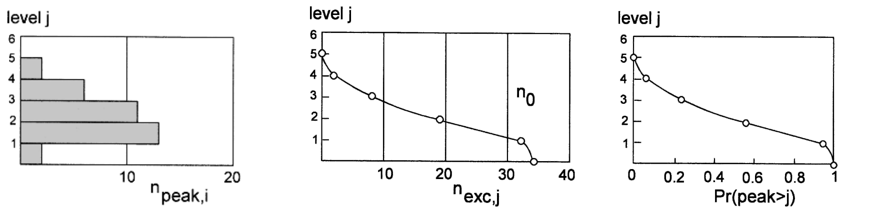

(a) Number of peaks in intervals

(b) Number of peaks exceeding level j

(c) Probability of exceeding level j

Fig. 9.7 Peak counting results of the load-time history sample in Figure 9.6.

Numbers are counted in Figure 9.6 for levels $j = 0$ to $j = 4$, see the numbers $n_{\text{exc},j}$ in the row to the far right of this figure. The number of peak values in an interval ($n_{\text{peak},i}$) is then obtained as the difference between the numbers of level crossings of the two enclosing levels of the interval:

$$n_{\text{peak},i} = n_{\text{exc},j=i-1} - n_{\text{exc},j=i} \tag{9.1}$$

These numbers have been plotted in Figure 9.7a, which is a histogram of the number of peak loads in the intervals. The numbers of peak values above load level j are plotted in Figure 9.7b. A curve is drawn through these counting results. These exceeding numbers are normalized in Figure 9.7c by dividing $n_{\text{exc},j}$ by the total number of peaks (n_0) above the zero reference level ($j = 0$), see Figure 9.7c. The values obtained are related to the probability of a peak value occurring above level j, or:

$$\text{Pr}\,(\text{peak} > \text{level } j) = \frac{n_{\text{exc},j}}{n_0} \tag{9.2}$$

In Figure 9.6, a short load-time history was used to illustrate the counting technique. A long load-time history with a stationary character will lead to an exceeding probability curve with a stationary character. In statistical terms, the curve becomes an estimate of the *probability function* of the occurrence of peak values. The bar chart of the number of loads in load level intervals is associated with the *probability density function.* Load spectra are usually presented as load exceeding curves as shown in Figure 9.7b. They must then be related to a certain time in service.

A second example of a load history is given in Figure 9.8. The load variation is no longer symmetric in this case, but a reference level can again be determined with alternating maxima and minima above and below this level respectively. Counting can occur in load intervals for the minima and maxima separately, which leads to two load spectra for the maxima and

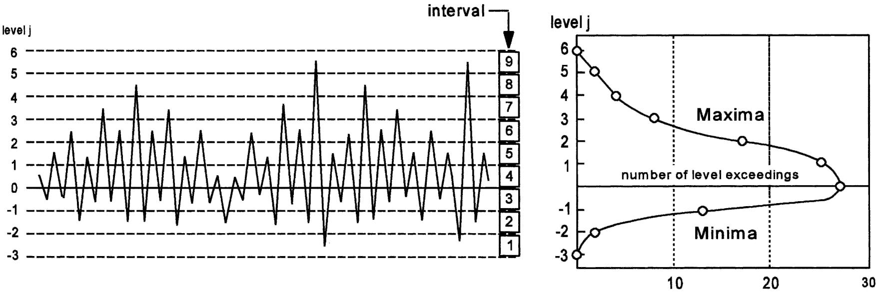

Fig. 9.8 A non-symmetric load-time history. Separate counts of maxima and minima.

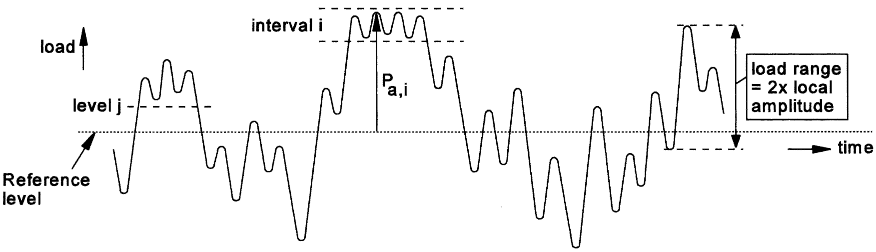

Fig. 9.9 An irregular load-time history.

minima as presented in Figure 9.8b. The number of maxima and minima must be equal (the number is 27 in Figure 9.8a). The two spectra for the maximum and the minimum peak values in Figure 9.8b give indications about the size of the positive and negative peak values, and about how often they occur. This information may be instructive for a first evaluation of the severity of a non-symmetric load spectrum, and also for comparing load spectra of different severities.

The two load-time histories in Figures 9.6 and 9.8 contain only maxima above the reference level and minima below this level. However, the situation is different for a more irregular load-time history as shown in Figure 9.9. In Figures 9.6 and 9.8, the number of positive level crossings of level j ($n_{\mathrm{exc},j}$) was equal to the number of peak values above level j. However, in Figure 9.9, level j in the first part of the load history is associated with one positive level crossings whereas the corresponding number of positive peaks larger than level j is equal to three. Actually, it is not difficult to see that the number of positive level crossings is equal to the number of maxima above that level reduced by the number of minima above that level. As a consequence, Equation (9.1) is no longer applicable and the numbers of peak values in an interval cannot be derived unambiguously from level crossing counts. Of course, the peak values can be counted in a number of intervals and the counting results can still be presented in statistical graphs. But it may be questioned whether this is meaningful. In Figure 9.9, four maxima are counted in interval i, but they are due to small load variations. These peak values cannot be associated with four loads with an amplitude $P_{a,i}$.

A load sequence as shown in Figure 9.9 is more irregular than the load sequences of Figures 9.6 and 9.8. The irregularity of a load-time history can be defined by an irregularity factor which is the ratio of the number of peak values and the number of level crossings of the reference level:

$$k = \frac{\text{number of peak values}}{\text{number of level crossings of the reference level}} \tag{9.3}$$

The irregularity factor is obviously equal to 1 for constant-amplitude loading, but also for a load-time history with an amplitude modulation in Figure 9.6. The factor remains equal to 1 in Figure 9.8 for the non-symmetric load-time history with alternately positive and negative load amplitudes. If the irregularity factor is equal to 1, the magnitude of load excursions with respect to the reference level can be indicated by a single load parameter. However, this is not possible for an irregular load-time history for which $k > 1$. The value of k in Figure 9.9 is 2.5 which implies a high irregularity. In such cases, an apparent need is present to consider load variations between successive peak values in terms of load ranges which is discussed later.

Flat and steep load spectra

If the irregularity of a load-time history is limited (i.e. with an irregularity factor not too much above 1), useful statistical data on peak loads can still be presented in the format of a one-parameter load spectrum. In such a case, the shape of the load spectrum is of interest. Two significantly different shapes are shown in Figure 9.10. As mentioned before in the discussion on Figure 9.7b, such spectra should be associated with certain periods in service, e.g. hours or years, or also the number of times of using the structure (missions). Load spectra should preferably cover long periods in order to be representative for the variability of the load-time history. The load level in the two fictitious spectra in Figure 9.10 (1000 hours in service) are expressed as a percentage of the maximum load occurring in that period. Figure 9.10 shows a steep load spectrum and a flat load spectrum. In a steep spectrum, the number of high loads is small and the number of low loads is large. As an illustration, high loads with a peak value exceeding 80% of the maximum

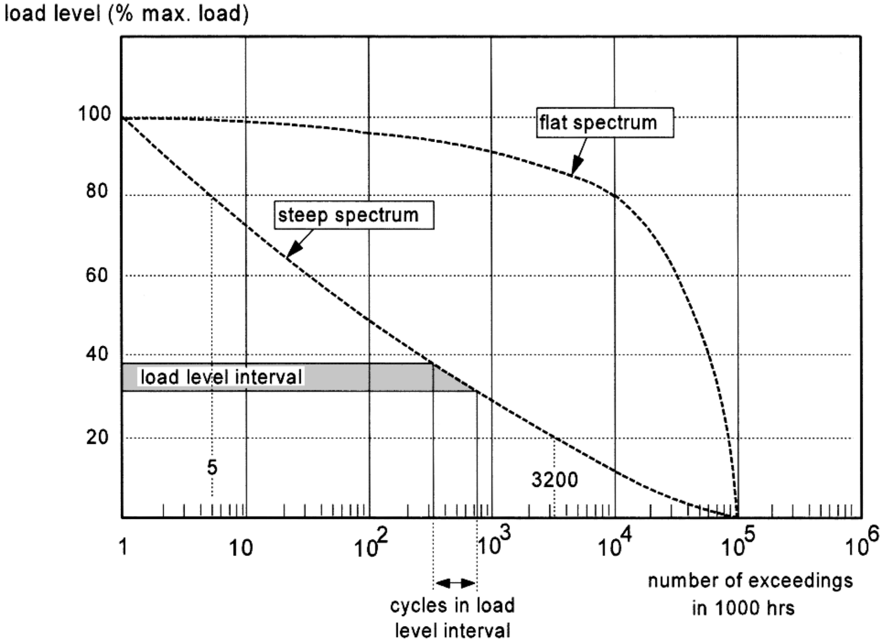

Fig. 9.10 Two different types of load spectra.

load of the steep spectrum in Figure 9.10 occur only five times, whereas the number of low loads with a peak value below 20% of the maximum load is 100000 – 3200 = 96800 cycles which is 97% of all cycles. The opposite is true for the flat load spectrum. Again in Figure 9.10, the 80% load level is exceeded 10000 times, whereas the number of small cycles below 20% of the maximum load is relatively small: 100000 – 85000 = 15000 cycles which is 15% of all cycles. Large and small cycles have special effects on fatigue as discussed in Chapters 10 and 11, see also Section 9.5.

Range counting methods

From a fatigue damage point of view, load amplitudes are more significant than mean loads. The amplitude is half the range between a minimum load and the subsequent maximum load. Load ranges represent important characteristic values of a load-time history exerted on a structure or applied in a fatigue tests. Load ranges of a load-time history can be counted, but since ranges are defined by a minimum and a maximum, a two-parameter counting methods must be adopted. Results can then be presented in matrix

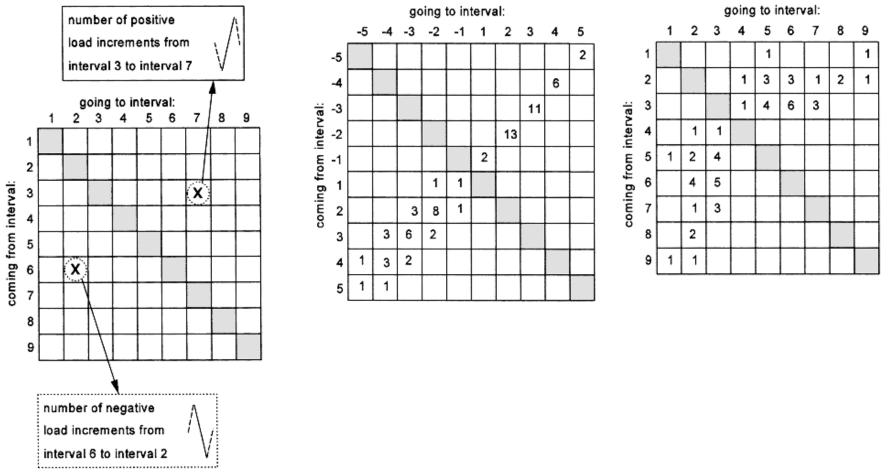

(a) Matrix presentation of bad ranges occurring between different load intervals

(b) Range countings of the load-time history of Figure 9.6

(c) Range countings of the load-time history of Figure 9.8

Fig. 9.11 Two-dimensional load range countings in matrix format.

format as is illustrated by Figure 9.11. A range is counted in the matrix at the corresponding interval in which the range was starting (listed at the left-hand side of the matrix) and the interval in which the range is completed (listed at the top side of the matrix). As indicated in Figure 9.11a, a positive load range coming from a minimum and going to a maximum, is counted in the upper right triangle of the matrix. Negative load ranges, coming from a maximum and going to a minimum, are counted in the lower left triangle of the matrix. The counting results of the load-history samples in Figures 9.6 and 9.8 are given in Figures 9.11b and 9.11c respectively. It should be noted that the counting results in Figure 9.11b are along a diagonal of the matrix. This should be expected because for this load-history (Figure 9.6) each peak load is followed by an opposite peak load of approximately the same magnitude. This is not true for the load history in Figure 9.8, which leads to more distributed counting results in the matrix of Figure 9.11c. The matrix is thus characteristic for the random nature of the load history. It is a two-parameter counting method, and for each range the mean value can easily be calculated because the minima and the maxima of the ranges are known. The accuracy is limited because counting of peak values does not indicate the exact location of a peak in an interval. However, smaller intervals can improve the accuracy.

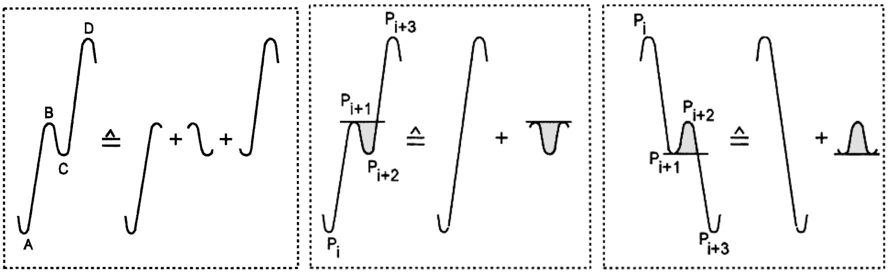

(a) Range countes (b) Rainflow counts (c) Rainflow counts

Fig. 9.12 Intermediate load reversal as part of a larger range.

The rainflow count method

In principle, range counting includes counting of all successive load ranges, also small load variations occurring between adjacent larger ranges. It might be thought that small load variations can be disregarded in view of a negligible contribution to fatigue damage. A fundamental counting problem arises if a small load variation occurs between larger peak values. This situation is illustrated in Figure 9.12. A two-parameter range counting procedure will count the ranges AB, BC and CD, and store this information in a matrix. Now, consider the situation that the intermediate range BC would not occur. Then, the large range AD would be counted only. Fatigue damage is related to load ranges. It should be expected that the fatigue damage of the large range AD alone is larger than for the three separate ranges AB, BC and CD. This has led to the so-called rainflow counting method of Endo [5].[12] The intermediate small load reversal BC is counted as a separate cycle and then removed from the major load range AD. This larger range can then be counted as a separate load range, see Figure 9.12b. If four successive peak values are indicated by P_i, P_{i+1}, P_{i+2} and P_{i+3}, the rainflow count requirement for counting and removing a small range from a larger range is

$$P_{i+1} < P_{i+3} \quad \text{and} \quad P_{i+2} > P_i \tag{9.4a}$$

If the intermediate small load reversal occurs in a descending load range, see Figure 9.12c, the requirement is

$$P_{i+1} > P_{i+3} \quad \text{and} \quad P_{i+2} < P_i \tag{9.4b}$$

[12] A similar eliminating concept for small intermediate ranges was described by Anne Burns in 1956 [6]. The Strain-Range-Counter developed by the Vickers aircraft industry was counting in accordance with this method.

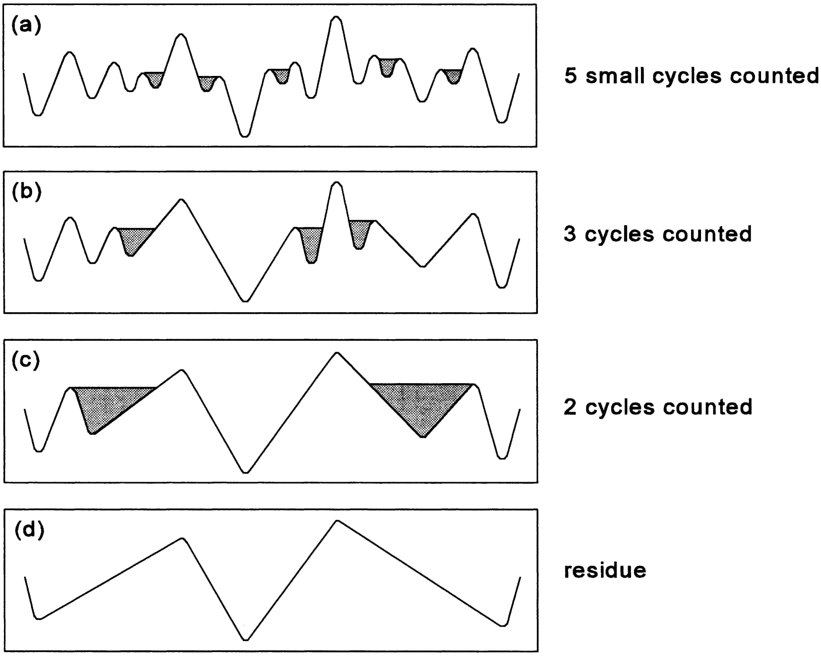

Fig. 9.13 Successive rainflow counts.

In words: the peak values of the intermediate small load reversal should be inside the range of the two peak values of the larger range. Successive rainflow counts are indicated in Figure 9.13. In Figure 9.13a five rainflow counts can be made. After counting and removing these small cycles, Figure 9.13b is obtained. In this figure again three rainflow counts can be made, but now of larger ranges. Removing these cycles lead to Figure 9.11c in which again two still larger load reversals can be counted and removed. In the final residue, Figure 9.11d, no further counts are possible. The ranges of the residue must be counted separately at the end of the counting procedure. The rainflow count results can be stored in a similar two-parameter matrix as discussed before (Figure 9.11).

The rainflow count procedure has found some support [7] by considering cyclic plasticity. A short load sequence is given in Figure 9.14a, which leads to counting two intermediate load reversals by the rainflow count method, as indicated in this figure. The corresponding plastic behavior is schematically indicated in Figure 9.14b, which could apply to local plasticity at the material surface during the initiation period, or to crack tip plasticity during crack growth. The intermediate load reversals $c1$ and $c2$ are causing hysteresis loops inside the major hysteresis of the major cycle between A and B. It is

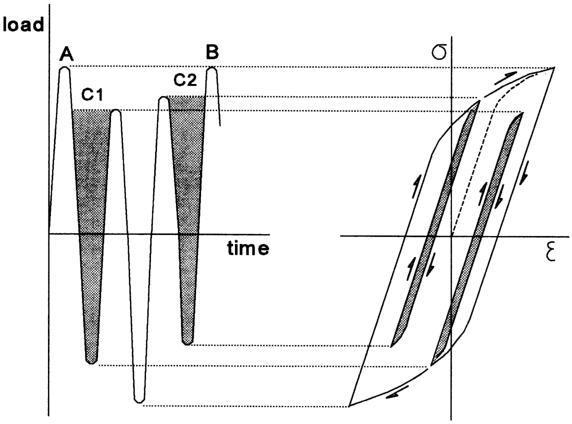

(a) Load history sample with two intermediate load reversals

(b) Corresponding plastic deformation loops

Fig. 9.14 Hysteresis loops associated with rainflow counts.

thus assumed that the intermediate plasticity loops do not affect the major loop. This reasoning gives somewhat speculative support to the rainflow counting method.

Some more comments on counting methods

As discussed in the previous text, statistical information of load-time history obtained by counting of level crossings, peak values, or ranges can be presented in a graph or a matrix. A graph represents a one-parameter distribution function while a matrix corresponds to a two-parameter distribution and thus gives more information. However, one significant aspect was not yet mentioned. Information about the sequence in which the counts were made is lost by these counting procedures. The matrix in Figure 9.11 collects numbers of ranges between successive peak values, but information about the sequence of the ranges is not obtained.

Some indirect information about sequences is retained in the rainflow count method. Each range counted by the rainflow procedure and stored in the matrix combines two peak values which may have been separated by intermediate load reversals in the original load-time history. However, these smaller ranges should have occurred between those two peak values in order to satisfy the rainflow count equation (9.4). Intermediate larger ranges did not occur because of the counting condition in the same equation. Anyway, the question must be considered whether the sequence is important

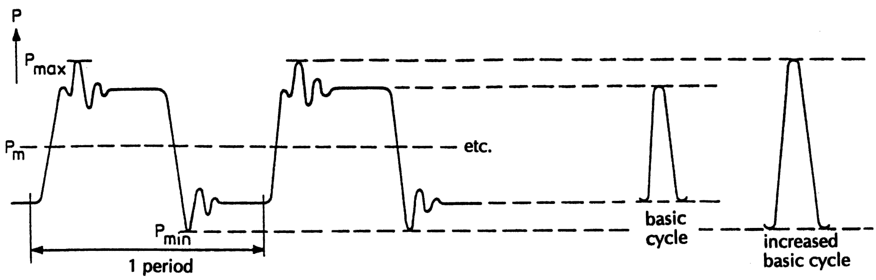

Fig. 9.15 Transient load fluctuations during on/off switching of machinery.

for fatigue predictions. The significance of sequences for fatigue damage accumulation is considered again in Chapters 10 and 11 on fatigue under variable-amplitude loading. Here, it should be emphasized that a most direct impression of a load-time history is obtained from records as presented here in Figures 9.6 and 9.8, and other ones discussed later.

The rainflow count method is generally suggested to give a better statistical reduction of a load time history defined by successive numbers of peaks and valleys if compared to the level crossing counts of Figures 9.6 and 9.8 and the range counts of Figure 9.11. Two main reasons for preferring the rainflow count method are: (i) an improved handling of small intermediate ranges, and (ii) an improved coupling of larger maxima and lower minima to range counts as will be illustrated below. In spite of this advantages, it cannot be said that the rainflow count method is fully based on rational arguments. It is easily recognized from Figure 9.13 that larger ranges counted by the rainflow method are separated by more intermediate smaller load ranges. The counting residue mentioned before consists of an increasing/decreasing series of positive peaks, and a decreasing/increasing series of negative peaks. These peaks may be separated by many intermediate peaks. It then becomes questionable whether counts of the residue are still meaningful for the evaluation of fatigue damage accumulation. It depends on the memory of the material during fatigue damage accumulation. The problem may be less serious for a flat spectrum with a large number of severe peak loads.

The significance of the basic idea of the rainflow counting method are illustrated by two simple examples. Figure 9.15 shows the load variation in a workshop machine due to switching on and off. The basic load cycle is a static block type load, but at the moment of switching some vibrational loads are introduced. The rainflow procedure will count several small load cycles, but instead of the deterministic static load cycle it also counts an increased basic load cycle between P_{max} and P_{min}, see Figure 9.15. Although the small

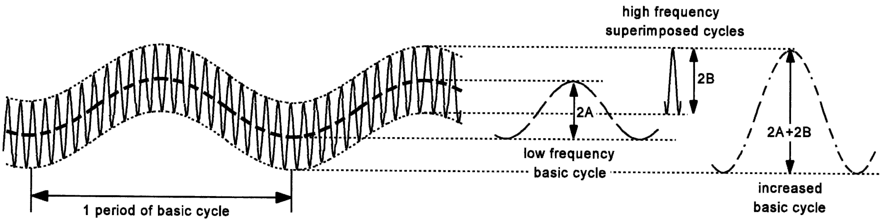

Fig. 9.16 High-frequency cyclic load superimposed on a low-frequency base line cycle.

vibrational load cycles could be practically harmless by themselves, they increase the severity of the basic load cycle. From a fatigue point of view, the material feels the increased basic cycle, and this increased load cycle is recognized by the rainflow counting method. A similar case was already discussed in relation to the superposition of random loads on a deterministic load cycle in Figure 9.5. The rainflow count method recognizes the largest cycle of the flight between the maximum peak in flight and the most severe downward load on the ground.

A second illustrative example is shown in Figure 9.16. A high-frequency load cycle (amplitude B) is superimposed on a low-frequency base line load cycle (amplitude A, frequency ω_1). According to the rainflow counting method, one cycle with an amplitude of $A + B$ will be counted in each period of the base line period, and that makes this cycle more damaging. This can be important depending on the damage done by the small superimposed high-frequency cycles. If ω_2 is much larger than ω_1, the number of the high-frequency cycles will contribute the major part to the fatigue damage, and the base line cycle is no more than a varying mean load, probably with a limited effect only.

Random Gauss process

Some types of random loads are caused by a stochastic random process. Turbulent air, in which an aircraft is flying, is supposed to be such a process. The same applies to random noise of a jet engine and water waves of the sea. It is often assumed that such processes are a random Gauss process which implies that the relevant variables have a normal distribution function (i.e. a Gaussian distribution). A random Gauss process is defined by a power spectral density function, $\phi(\omega)$, which fully describes its statistical properties. Examples are shown in Figure 9.17a. The power spectral density function shows how the energy of the signal is distributed as a function of

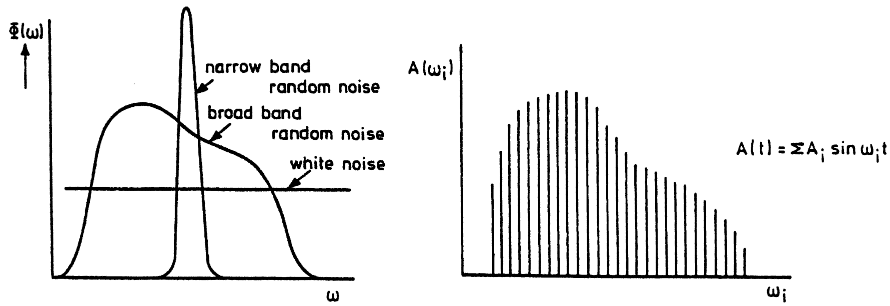

(a) Different types of energy density functions of a random signal

(b) Fourier series approximation of a random signal

Fig. 9.17 Energy density functions to define a random load Gauss process.

the frequency ω. This concept can be understood by considering a Fourier series with a very large number of terms and small differences ($\Delta\omega$) between the frequencies of successive terms, and coefficients A being a function of ω, see Figure 9.17b. The load-time history is then

$$A(t) = \sum A_i \sin(\omega_i t)$$

This sum gives a signal $A(t)$ which is approximately similar to random noise. It becomes a real random Gauss signal if $\Delta\omega \rightarrow 0$. The energy is proportional to the square of the amplitude:

$$\Phi(\omega) \propto [A(\omega)]^2$$

Two examples of a random Gauss signal and the corresponding power spectral density functions are shown in Figure 9.18. In Figure 9.18a, the energy is concentrated in a narrow frequency band and as a result the load-time history is somewhat similar to an amplitude modulated signal, in this case with a random modulation. This *narrow band random loading* is typical for resonance systems, which predominantly respond at one single resonance frequency if activated by some external random process covering a wider frequency band. The structure acts as a frequency filter to the excitation. The second example in Figure 9.18b shows a random signal covering a wider frequency band and the corresponding broad band random load signal shows a higher degree of irregularity. It was shown by Rice [9] that the distribution function of the peak values of a random Gaussian signal can mathematically be derived from the spectral density function $\Phi(\omega)$. This is also true for the irregularity factor k defined earlier as the

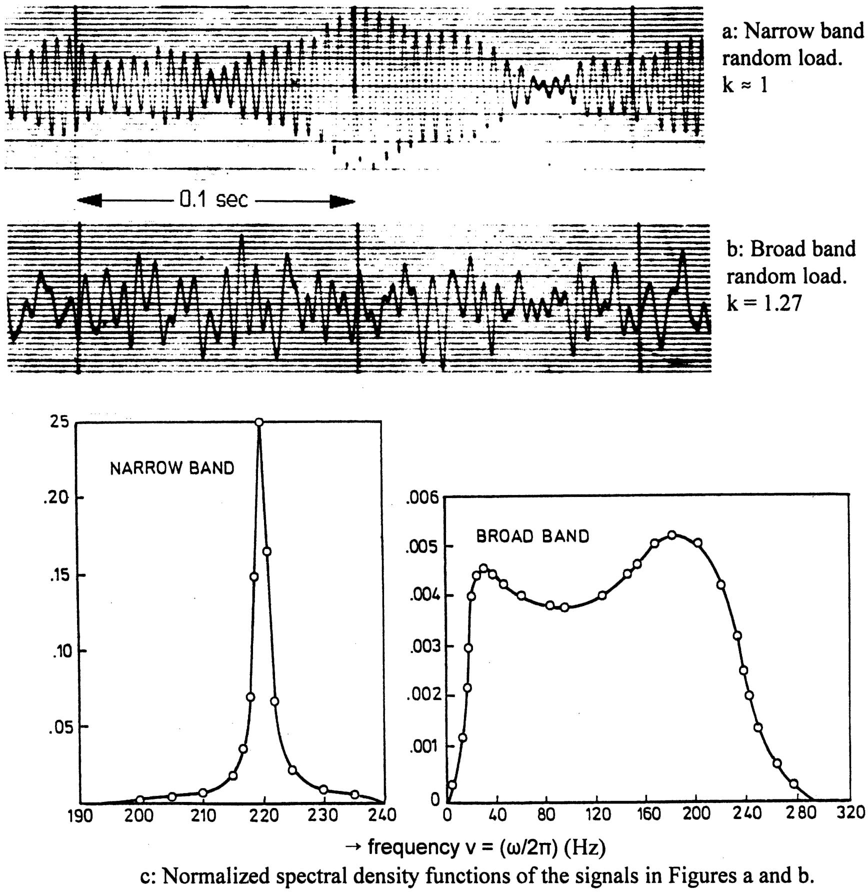

Fig. 9.18 Two records of random load and the corresponding spectral density functions [8].

ratio of the number of peaks and the number of zero-crossings (crossing the level $A = 0$). As might be expected, this factor is almost equal to 1 for narrow band random loading, whereas it is larger for more irregularly varying signals, see Figure 9.18b. A mathematically closed form solution for distribution functions of ranges cannot be derived from the spectral density function.

The application of power spectral density techniques to the dynamic behavior of a structure is of interest. If a random Gaussian load is applied to a linearly elastic structure, then the stress in the structure is also a random Gaussian phenomenon. The spectral density function of the stress can be calculated from the spectral density function of the external load by using a transfer function, depending on the elastic properties of the structure. This problem of applied dynamics is outside the scope of the present discussion. However, it can be useful for discussions on random fatigue load spectra to know whether the loads are narrow band or broad band phenomena.

9.4 Determination of load spectra

Different types of fatigue loads and description techniques of load-time histories were presented in Sections 9.2 and 9.3 respectively. The question now is: How can a load spectrum be determined if the fatigue performance of a structure must be investigated? Two obvious approaches are: (i) by analyzing the use of the structure, and (ii) by measuring the loads on the structure if the structure, or a similar previous structure, already exists. In Section 9.2, five examples of structures under fatigue loads were discussed, which led already to several questions. The principal question is: which cyclic loads will occur? Sometimes, the categories of loads follow directly from the purpose of the structure, e.g. pressurization cycles of a vessel, and train passages on a railway bridge. The question is more difficult for moving vehicles. Different problems arise if vehicles can be used for several purposes under various conditions. As an example, this has been recognized for trucks to be used in countries with poor roads. The trucks for these countries are made stronger by the automotive industry, stronger than for countries with a modern road system. Stronger implies a more heavy truck and thus less cargo capacity.

Knowledge of relevant load spectra is also depending on experience of an industry with respect to the performance of their products in service. Much has been learned from case histories of fatigue failures occurring in service and accident investigations. In any case, the designer must use his imagination to see how the structure can be used. Perhaps he should consider abusive use as well. Depending on the consequences of fatigue failures in service, a worst case approach must be considered.

In general, it is difficult to define straight forward procedures how to obtain load spectra to be used for fatigue life predictions, and also for supporting experimental work if that appears to be necessary. Two steps in the load spectrum evaluation may be recognized: first, a qualitative approach, and second, a more quantitative approach.

9.4.1 The qualitative approach

Figure 1.1 shows a broken front-wheel of a heavy motorbike. The fracture surfaces of the spokes clearly indicated fatigue failures. The front wheel collapsed during braking before a railway level crossing which was closed. The police-officer driving the motorbike survived. It turned out that similar failures occurred in the same motorbikes of the police in other countries. The failure was not an incidental case, but a symptomatic one. The question then is, what is so special about the use of these motorbikes by the police? Analysis showed that the police were using the brakes very often, which led to a heavy moment on the front-wheel spokes even if the driving speed was low. Apparently, a predominant fatigue load occurs for a special group of users of the motorbike, but not for all users. It illustrates that different groups of users of a structure must be considered.

A subsequent question then is: which utilization is the most severe one on which a fatigue analysis should be based? The answer to this question can depend on economic and safety consequences of fatigue failures in service. The variety of economic consequences can be large. Related aspects are: repairs, replacements, inspections, structure not to be used before some remedial efforts are introduced, etc. Financial liability as well as the reputation of a product of the industry can also be involved. Sometimes consequences are self-evident. A pressure vessel should not explode as a result of fatigue cracks. Cables of a passenger lift in the mountains should never fail. In any case, designing against fatigue requires consideration of all possible *scenarios* of how a structure might be used and how it can fail by fatigue.

In general, the designer knows more or less the type of loads to which his structure is subjected in service, at least the regular type of loads. As an example, a list of loads on a transport aircraft is shown in Table 9.1 which also includes some numerical information. It should be noted that the data illustrate possible orders of magnitudes only. The numerical data can vary within fairly wide margins, depending on the type of aircraft and how it is going to be used. Moreover, the list of types of fatigue loads in the table is not necessarily complete.

Information on load spectra for aircraft is relatively abundant, but for various structures it may be difficult to set up similar lists. The type and character of known fatigue loads in service can usually be determined reasonably well. However, statistical information about the load spectra in

Table 9.1 Global information about different types of loads on an aircraft structure.

Type of load	Character	Number of cycle in the design life time	Period of 1 cycle
ground-air-ground transition cycle	deterministic	10^3 to 10^5	10 min to 10 hrs
pressure cycle of the cabin		10^3 to 10^5	10 min to 10 hrs
maneuvers		4×10^3 to 4×10^5	10 sec to 3 min
turbulence (gusts)	random	10^5 to 10^6	0.1 sec to 10 sec
taxiing loads		10^5 to 10^7	0.05 sec to 1 sec
acoustic loads		10^7 to 10^8	0.001 sec to 0.01 sec

many cases is non-existent. Measurements, quite often with strain gages, can then be most informative.

Buxbaum [10] presented an instructive example of measurements of the bending moment in an axle-spindle of a motor car, see Figure 9.19. The upper record suggests that two types of loads are superimposed. By a separation technique, it was shown to consist of a maneuver type of loading and a random vibrational load due to roughness of the road. Rainflow counts of the upper record can give a useful representation for fatigue damage analysis, but the separated signals give a much better impression of the two different types of loads acting simultaneously on the structure. Moreover, a design

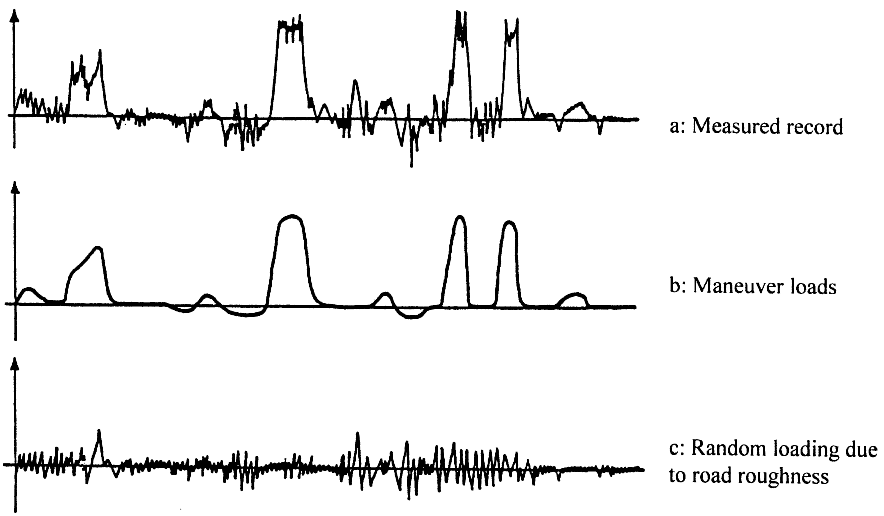

Fig. 9.19 Load record of an axle spindle of a motor-car, separated in two different types of loads [10].

modification for improving the fatigue performance of a structure may be effective for one type of loading, but not necessarily for other ones. For instance, a change of the resonance frequency of a structure and introducing more damping can significantly reduce the stress spectrum induced by random vibrations, whereas the stress spectrum of maneuver type loads is not substantially changed. The relation between the external load spectrum and the stress spectrum in the structure (the transfer function) can be different for different types of loads, in particular for random vibration loads compared to deterministic maneuver loads. The dynamic response of the structure should then be considered.

Unfortunately, fatigue failures occurring in service often have shown that not all significant fatigue loads on a structure were known before. An example is described by Griese et al. [11]. Fatigue problems occurred in the drive shaft of a heavy-plate rolling machine. The torsion moment on the shaft was measured. The results presented in Figure 9.20 show that significant load cycles occurred at the moment that the plate was entering the rollers, and also when the plate was leaving the rollers. Probably, such severe extra load cycles would not occur if rolling could be done slowly, almost quasi-statically. But slow rolling will be undesirable from an economic point of view. Anyway, it illustrates that it can be difficult to anticipate all loads which can occur in service.

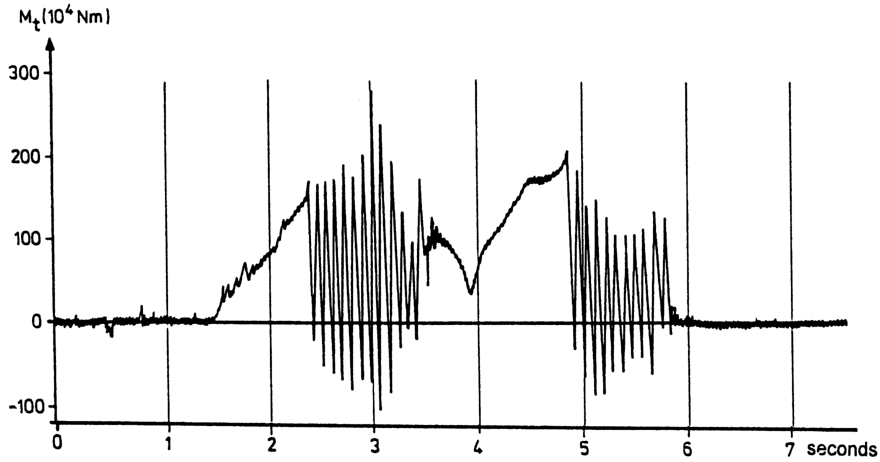

Fig. 9.20 Measured torsion moment on a driving shaft of a rolling machine for heavy steel plates [11].

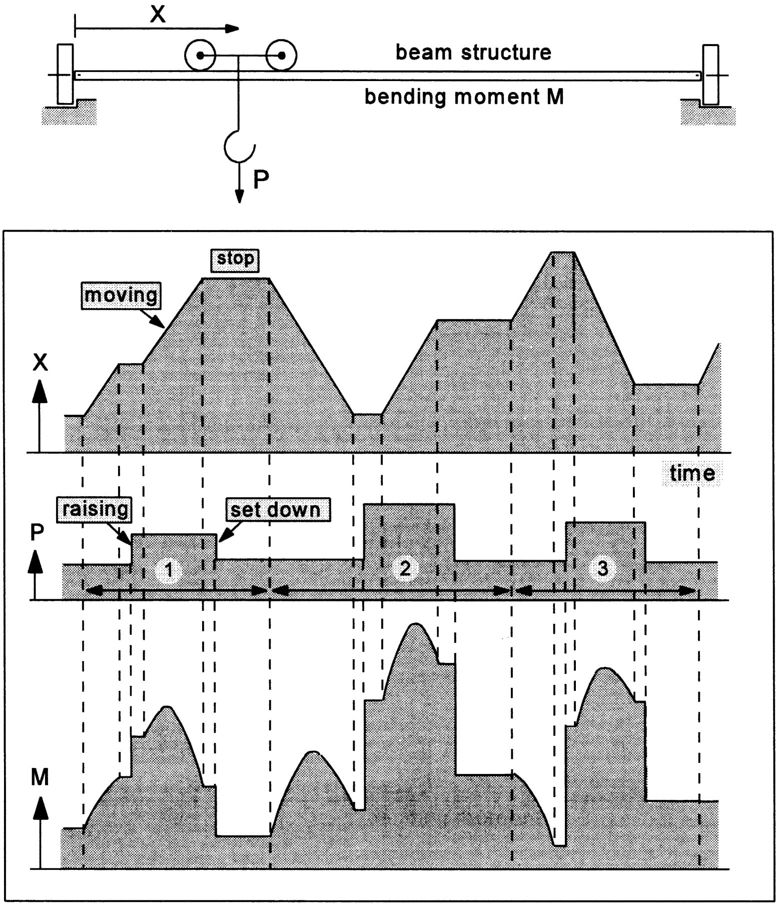

Fig. 9.21 Calculated load history for a traveling crane in a production hall [12].

9.4.2 The quantitative approach

Quantitative assessments of load spectra is a problematic issue for most structures. A simple case is a pressure vessel with known pressure variations and no other load fluctuations. Another illustrative example with still relatively simple conditions was discussed by Weiss [12]. He considered a traveling crane in an industrial production hall used for transportation of heavy items of different weights to various locations (x, y) in the hall, see Figure 9.21. A part with a certain weight is lifted by the crane and then transported to another location. The structure to be considered is the beam spanning the two rolling supports. The bending moment in this beam (M) depends on the weight (P) and the location of the lifting cart on the beam (x).

The top graph in Figure 9.21 shows that the crane is moving and makes stops for lifting up a weight or putting it down. The bending moment can be calculated from the weight P and the crane location x, see the lower graph of Figure 9.21. It should be noted that the three transport segments in this figure (1, 2 and 3) give rise to four load cycles. This example shows that the bending load cycles can be calculated, but it requires detailed information regarding the usage of the crane. Moreover, the load spectrum thus obtained presumes that no transient loads occur during the moment of lifting a weight or putting it down. Dynamic conditions are obviously more complex for a large outdoor crane with more kinematic possibilities, operating in a windy climate, and meeting inertia loads of moving parts. Measurements of load-time histories with strain gages are recommended.

With some imagination about how a structure will be used, a list can be made of the various types of cyclic loads acting on the structure. An example of such a list was already given in Table 9.1 for an aircraft structure for which predictions on load-time histories have received much attention. This certainly was stimulated by some dramatic aircraft crashes caused by fatigue cracks. The analysis starts with a so-called *mission analysis*, which implies that imaginary flights are made according to expectations for a transport aircraft, a military aircraft, or some other type of aircraft. The deterministic loads (maneuvers) often allow calculations about the magnitudes of the cyclic loads. It is much more difficult for random loads due to gusts and taxiing. Calculation techniques have been developed for the dynamic response of the structure, but the analysis is difficult, also because damping (aerodynamic damping for the wing) is a complication. If it is possible, calculations should be supplemented by measurements on an aircraft in service. Two samples of strain gage records for a wing in turbulent air are presented in Figure 9.22. The record of aircraft A with a slender wing and two jet engines attached to each wing shows vibrations with a frequency in the order of 2 Hz (period $\approx 1/2$ sec). This frequency corresponds to the first mode of wing bending vibrations. Such vibrations are hardly observed in the record for aircraft F with a relatively high bending stiffness and only one turboprop engine on each wing. The dynamic response of the wing structure is affecting the stress spectrum of the wing structure. Similar problems apply to the load records in Figure 9.19 for the motor-car axle. It is difficult to predict the random bending moment variation invoked by road roughness, partly because the statistical data on surface roughness may be questionable, but also because the dynamic response is a complex phenomenon. In addition, it is not really easy to predict the maneuver component of the car load history.

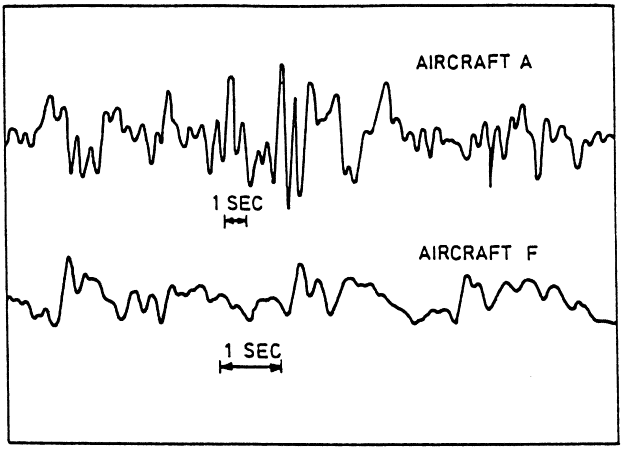

Fig. 9.22 Strain gage records of wing bending for two types of aircrafts flying in turbulent air [2].

Because quantitative evaluations of load spectra for a fatigue critical location in a structure can offer significant problems, a need for load-history measurements is easily recognized. Such measurements are not necessarily complicated. Some types of sensors can be used, but strain gages are most popular. Strain gages can be sealed very well and thus also be used over long periods in different environments. How to sample data depends on the problem to be investigated. If the purpose is to know more about the characteristic nature of certain load variations, then a continuous analogue record can be very instructive, see the samples in Figures 9.19, 9.20 and 9.22. However, if the nature of the loads in reasonably well understood, but the number and magnitude of the cycles are not very well known, then counting peaks and troughs is most useful. Small sized equipment and software for a counting analysis are commercially available for that purpose. It can provide the data in the two-parameter matrix format discussed before (Figure 9.11). It is also possible to store the full sequence of the peaks and troughs. Rainflow counting can be done, as well as other counting methods. Equipment was also developed for telemetric measurements on moving vehicles and rotating parts.

A typical problem is offered by the replacement of old bridges which may be older than 100 years, but which were originally designed with very high safety factors [13]. Measurements of load spectra are then essential to consider the question whether the bridge is still good enough for the present time (cheap solution), or should it be replaced by a new one (expensive solution).

Another illustrative example occurred when NLR (National Aerospace Laboratory, Amsterdam) wanted to test new load-history counting equipment. As a trial experiment, some strain gages were bonded on the wing struts of a training glider. Launching occurred by a winch. After landing, the glider was towed by a jeep to the original launching position on the airstrip. The measurement results, immediately available after the flight, indicated that just a single flight was sufficient to show that the larger cyclic loads did not occur in flight, but during towing of the glider after landing, due to transportation over a rough terrain.

Similar measurements on a new structure can rapidly and easily produce useful information about load spectra. It can show how a structure is really used. Furthermore, load spectrum measurements applied on an existing structure already in service for several years enables a comparison between the present load spectrum and the spectrum assumed in the design stage of the structure. Measurements are also carried out for load spectrum monitoring of military aircraft in order to analyze problems about life limitations and inspection periods. Indications about safety margins are then obtained.

9.5 Service-simulation fatigue tests and load spectra

Predictions on fatigue life and crack growth under Variable-Amplitude (VA) fatigue loading are discussed in Chapters 10 and 11 respectively. It will be explained that predictions made by the well-known Miner rule are not reliable, partly because of shortcomings of this rule, and also due to uncertainties about the required S-N curves. Service-simulation fatigue tests should then be considered. The load-time history in a service-simulation fatigue test must be a valid simulation of load histories which can occur in service. The problem is that the time scale in the test cannot be the same as in service because it would require an extremely long time for a single test. Some acceleration of the test is necessary in most cases. This may introduce a problem if some time-dependent phenomenon can effect the fatigue process.

The load-history sample in Figure 9.20 for a driving shaft of a rolling machine shows relatively fast cycles with a cyclic frequency of about 10 Hz, but most of the time the load is zero. If time-dependent phenomena do not affect fatigue, the load-history in Figure 9.20 can be compressed to the load

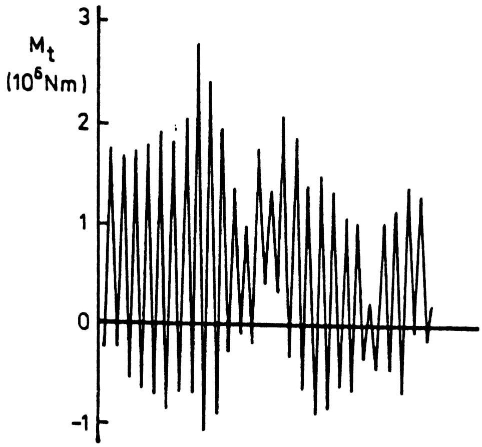

Fig. 9.23 Time compressed representation of the load history in Figure 9.20.

history shown in Figure 9.23, which can easily be applied in a computer controlled fatigue test.

A similar reduction of the time scale is adopted for fatigue tests of aircraft structures. The flight load profile for a single flight shown in Figure 9.5 in reality covers a period of 1 to 10 hrs, which is fully unacceptable for a service-load-simulation fatigue test. Time compression is obtained by applying all load variations in a short time, but maintaining the sequence of the successive maxima and minima, see Figure 9.24. Also the numerous taxiing loads may be omitted because they are supposed to have a negligible effect on fatigue in view of the low stress levels. However, the minimum load occurring during taxiing, the touch-down load in Figure 9.5, is maintained as the minimum load of the flight. This is necessary to obtain still the same fatigue damage of a flight according to a rainflow analysis of the load sequence.

Although a representative sequence of peaks is applied in a service-simulation fatigue test, the test in general will be an accelerated test. If fatigue in service occurs in a corrosive environment, results of service-simulation fatigue tests can be too optimistic. This problem is considered again in later chapters (Chapters 13, 16 and 20).

Service-simulation load histories in fatigue tests in most cases imply that a rather complex sequence of maxima and minima must be applied to a specimen or a structure. Fortunately, it is possible to apply complex load sequences in modern closed-loop electro-hydraulic fatigue machines which were introduced around the early 1970s. Such load sequences

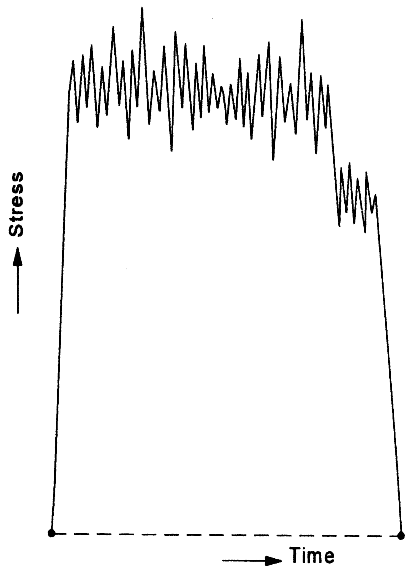

Fig. 9.24 Time compressed representation of the load history in Figure 9.5.

could not be realized in the older open-loop fatigue machines, which at best allowed block-program fatigue tests, discussed in Chapter 10. However, block-program tests are not recommended any more. Initially, service-simulation fatigue tests were more widely used for aircraft fatigue problems. These tests are also called *flight-simulation fatigue test* because a valid simulation requires flight-by-flight load sequences. As an example, a load history in such a test is shown in Figure 9.25. It applies to a civil aircraft wing structure. The full sequence includes 10 different types of flights. The stress-history was characterized by one specific stress level, for which the mean stress in flight (S_{mf} in Figure 9.25) was chosen. As discussed before, this load history is a combination of deterministic ground-air-ground cycles with superimposed gust loads (air turbulence) in flight. The ground-air-ground cycle can be calculated. The gust loads have to be derived from gust load statistics. Gust load spectra have been measured over long periods in service. The spectra are available as exceeding curves of the type shown in Figure 9.10 as a steep spectrum. Such a spectrum has to be broken down in spectra for different weather conditions occurring in different flights. It requires expertise about how this can be done in a statistically acceptable way [15].

Load-time histories for other types of structures require a similar analysis of the various missions of the structure in order to establish a

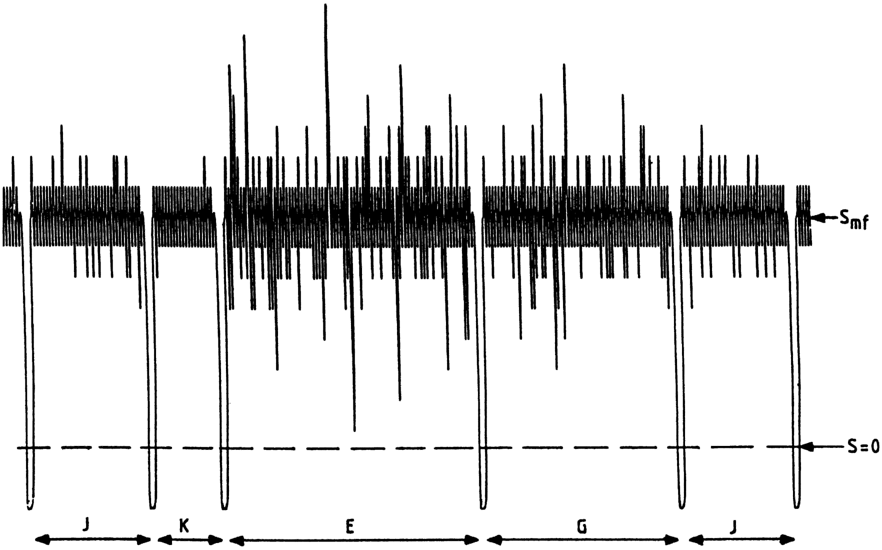

Fig. 9.25 Sample of a load history applied in flight-simulation fatigue tests [14]. Load spectrum of the Fokker F-28 wing structure. Five flights are shown with gust loads corresponding to different weather conditions.

simulation of load sequences as they would occur in reality. Obviously, load measurements in service can give most useful information for this purpose. Service-simulation fatigue tests are now carried out by various industries for several purposes discussed in Chapter 13.

If the load spectrum to be used in a service-simulation fatigue tests is available, problems can arise for a steep spectrum. The previous discussion on Figure 9.10 has revealed that a steep spectrum contains numerous low-amplitude cycles and a small number of high-amplitude cycles. If all low-amplitude cycles have to be included in a service-simulation fatigue test, the duration of the test would be very long. Very small cycles are therefore omitted from the load-time history in view of time efficiency. However, small cycles can contribute to fatigue damage, also when the amplitude is below the fatigue limit. Empirical evidence of representative specimens should give indications on this issue.

At the other end of a steep spectrum, the number of load cycles with a large amplitude is low. These cycles can considerably increase the fatigue life by introducing favorable residual stresses at notches. If the steep spectrum applies to wing bending of a transport aircraft, the high-amplitude gust loads occur in a flight in a most severe storm. Some aircraft of a fleet will meet this storm occasionally, but other aircraft will not. The fatigue life of the latter ones will be shorter. It is for this reason that the high-amplitude cycles in flight-simulation tests are truncated[13] to a lower amplitude level in order to avoid unconservative test results. The choice of the truncation level is a delicate question also for other types of structures subjected to a steep load spectrum. Fortunately, the problems of low-amplitude and high-amplitude cycles are much less important for a flat load spectrum. The topics are addressed again in Chapters 10 to 13.

9.6 Major aspects of the present chapter

The major aspects of load-time histories and load spectra discussed in this chapter are summarized below:

1. A load history applied to a structure in service is characterized by a sequence of successive maxima and minima (peaks) of the load on the structure. A load spectrum is a statistical representation of these maxima and minima, obtained by counting the numbers of peak values in load intervals, or counting the number of exceedings of load levels. The data can be presented in tables or graphs in which the magnitude of the load is indicated by a single load parameter. One-parameter load spectra can be instructive for general impressions of the spectrum severity and comparing load spectra of different severities.
2. Counting of load ranges between successive maxima and minima is also possible with results collected in a matrix. This is a two-parameter statistical representation of a load history which provides more information than a one-parameter counting method. The matrix gives information about load ranges between successive maxima and minima, but information about the sequence of these ranges is lost.
3. The rainflow count method is a range count method which counts intermediate smaller ranges separately. The rainflow count method should be preferred for a statistical analysis of load-time histories because it is more realistic in considering the fatigue damage of combined maximum and minimum loads.
4. Characteristic classifications of loads in service are: deterministic loads (especially maneuver type loads) and stochastic loads (in particular

[13] The terminology used here refers to truncation of high-amplitude cycles and omission of low-amplitude cycles. In the literature, these concepts are also called clipping of high-amplitude cycles and truncation of the low-amplitude tail of a load spectrum, respectively.

random loads). Another classification is stationary load spectra versus non-stationary load spectra.

5. Narrow band random loading looks like an amplitude modulated signal. Broad band random load has a more irregular character.
6. Continuous load-time records are most informative to show characteristic features of the load history which are not easily deduced from load counting results.
7. Load spectra for structures can vary from very simple (e.g. almost constant-amplitude loading of a pressure vessel) to rather complex (e.g. superposition of different types of loads from different sources with varying intensities and probabilities of occurrence).
8. Load spectra are essential for the analysis and predictions of fatigue critical structures. The spectrum of the stress in the structure is not linearly related to the load spectrum on the structure, depending on the dynamic response of the structure on external loads.
9. Assessments of load spectra for a structure should start with listing all types of loads occurring in service and their characteristic properties. Quantitative assessments of the spectra can be difficult due to lack of information. Load measurements should then be considered for which well developed techniques are available.
10. Quantitative information on load histories is also essential for planning service-simulation fatigue tests.

References

1. Private information Mr. van Maarschalkerwaart, Dutch Railways.
2. Schijve, J. *The analysis of random load-time histories with relation to fatigue tests and life calculations*. Fatigue of Aircraft Structures, 2nd ICAF Symposium, W. Barrois and E.L. Ripley (Eds.). Pergamon Press (1963) pp. 115–149.
3. Haibach, E., Fischer, R., Schütz, W. and Hück, M., *A standard random load sequence of Gaussian type recommended for general application in fatigue testing; its mathematical background and digital generation*. In: Fatigue Testing and Design. Vol. 2, Soc., Environmental Engineers, London (1976), pp. 29.1–29.21.
4. Schütz, W., *Standardized stress-time histories: An overview*. Development of Fatigue Load Spectra, STP 1006, ASTM (1989), pp. 3–16.
5. Matsuishi, M. and Endo, T., *Fatigue of metals subjected to varying stress – Fatigue lives under random loading*. Preliminary Proc. of the Kyushu District Meeting, The Japan Society of Mechanical Engineers (1968), pp. 37–40 [in Japanese].
6. Burns, A., *Fatigue loadings in flight: Loads in the tailplane and fin of a Varsity*. A.R.C. Technical Report C.P.256. London (1956).
7. Dowling, N.E., *Mechanical Behavior of Materials. Engineering Methods for Deformation, Fracture, and Fatigue*, 3rd edn. Prentice Hall (2006).

8. Hillbery, B.M., *Fatigue life of 2024-T3 aluminum alloy under narrow- and broad-band random loading*. ASTM STP 462 (1970), pp. 167–183.
9. Rice, S.O., *Mathematical analysis of random noise*. Bell System Tech. Journal, Vols. 23 and 24, (1944 and 1945).
10. Buxbaum, O., *Random load analysis as a link between operational stress measurement and fatigue life assessment*. ASTM STP 671 (1979), pp. 5–20.
11. Griese, F.W., Schöne, G., Schütz, W. and Hück, M., *Crack growth in torsion loaded axles of rolling machines during production*. Stahl und Eisen, Vol. 99 (1979), pp. 193–198 [in German].
12. Weiss, M.P., *Simulation and monitoring of loads in crane beams*. ASTM STP 671 (1979), pp. 208–221.
13. Yamada, K. and Miki, C., *Recent research on fatigue of bridge structures in Japan*. J. Construst. Steel Res., Vol. 13 (1989), pp. 211–222.
14. Schijve, J., Jacobs, F.A. and Tromp, P.J., *Fatigue crack growth in aluminium alloy sheet material under flight-simulation loading. Effect of design stress level and loading frequency*. Nat. Aerospace Lab. NLR, TR 72018, Amsterdam (1972).
15. de Jonge, J.B., Schütz, D., Lowak, H. and Schijve, J., *A standardized load sequence for flight simulation tests on transport aircraft wing structures*. Nat. Aerospace Lab. NLR, TR 72018, Amsterdam (1973). Also: Laboratorium für Betriebsfestigkeit LBF, Bericht FB-106 (1973).

Some general references

16. Murakami, Y., Mineki. K., Wakamatsu, T. and Morita, T., *Data acquisition by a small portable strain histogram recorder (Mini-Rainflow Corder) and application to fatigue design of car wheels*. Fatigue Design 1998, ESIS Publication 23, Elsevier (1999), pp. 373–383.
17. Heuler, P. and Schütz, W., *Standardized load-time histories – Status and trends*. In: Low Cycle Fatigue and Elasto-Plastic Behaviour of Materials. Elsevier (1998), pp. 729-734.
18. Rice, C.R. (Ed.), *SAE Fatigue Design Handbook*, 3rd edn. AE-22, Society of Automotive Engineers, Warrendale (1997).
19. Murakami, Y. (Ed.), *The Rainflow Method in Fatigue*. The Tatsuo Endo Memorial Volume. Butterworth Heinemann (1992).
20. Potter, J.M. and Watanabe, R.T. (Eds.), *Development of Fatigue Loading Spectra*. ASTM STP 1006 (1989).
21. Buxbaum, O., *Fatigue Strength in Service*. Verlag Stahleisen mbH, Düsseldorf (1986) [in German].
22. *Standard Practices for Cycle Counting in Fatigue Analysis*. ASTM Standard E 1049-85 (1985).